# Passive device based on plastic optical fibers to determine the indices of refraction of liquids

Joseba Zubia, Germán Garitaonaindía, and Jon Arrúe

We have designed and measured a passive device based on plastic optical fibers (POF's) that one can use to determine the indices of refraction of liquids. A complementary software has also been designed to simulate the behavior of the device. We report on the theoretical model developed for the device, its implementation in a simulation software program, and the results of the simulation. A comparison of the experimental and calculated results is also shown and discussed. © 2000 Optical Society of America

*OCIS codes:* 060.2370, 060.2340, 250.5460, 120.4570.

## 1. Introduction

Fiber optics has been a subject of considerable attention since it was discovered during the 1960's that optical fibers are useful transmission media. The reason for this interest lies not only in the applicability of this medium to communication systems but also in the great number of fundamental aspects that make this medium attractive for theoretical research.

Although plastic optical fibers (POF's) have been available as long as glass fibers, most studies until a few years ago were focused on glass optical fibers. A POF does not have such good transmission properties as its silica counterpart, but it is easier to handle and is cheaper;[1] It is suitable for use in short-haul links, and the new graded-index POF[2,3] can be used even at high-speed data rates.

For these reasons, many efforts have been devoted to studies of the properties of POF's. One of the most active fields in this area is that of the fiber optic sensors.[4–10] However, despite the considerable research that has already been done, there are a many POF-based sensors that require systematic and more-detailed study.[11–13] Specifically, there have been few reports of the application of POF's as refractive-index sensors.[14]

In this paper we report on the design, simulation, and experimental results of an inexpensive passive device based on a POF to measure the indices of refraction of liquids. We show that the design device can work in either of two ways: by having drops of liquid deposited on it or by being entirely submerged in the liquid. With these two modes of operation we get accuracies of $2 \times 10^{-3}$ and $5 \times 10^{-3}$, respectively, for indices of refraction of 1.42–1.52, which is good enough for some of the most popular industrial applications. The device has been applied to liquids such as oils, detergents, and juices.

We begin the paper with an explanation of the structure of the device as well as of the simulation model. We use the model to explain our experimental results, which are similar to those predicted by the simulation. At the end of the paper we summarize the main conclusions of this work.

## 2. Structure and Model of the Refractometer

To make the device we used a step-index POF with $n_{co} = 1.492$ and $n_{cl} = 1.417$. This fiber was inserted into a cast of polyester resin to facilitate the polishing that is necessary if the core is left uncovered [Fig. 1(a)].[15] The parameters chosen to characterize the device and its operation are [Fig. 1(b)]: $L$, the length of the polished core; $\delta$, the height of the liquid deposited on the device; $\rho$, the radius of curvature of the fiber; $n_s$, the index of refraction of the liquid; and $d$, the distance between the axis and the polished surface of the fiber.

To simulate the behavior of the passive device we use the ray-tracing method by placing a series of foci at the input, as Fig. 2 shows.[14,15] We calculate the ray paths through the structure up to the output end by taking into account the propagation properties of POF's as well as symmetry considerations.

We characterize the emitting source by modifying

The authors are with the Departamento de Electronica y Telecomunicaciones, ETSII y IT, Alameda de Urkijo s/n, 48013 Bilbao, Spain. The e-mail address for J. Zubia is jtpzuzaj@bi.chu.es.

Received 21 May 1999; revised manuscript received 12 October 1999.

0003-6935/00/060941-06$15.00/0

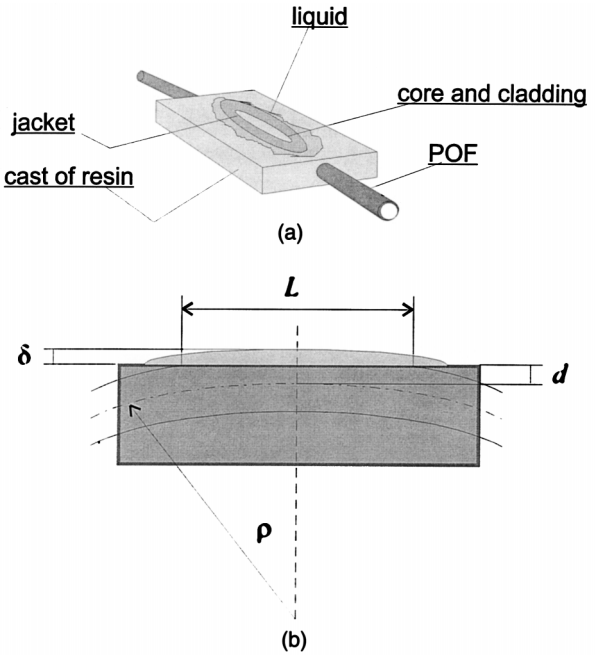


Fig. 1. (a) Structure of the device. (b) Parameters that characterize the behavior of the device.

the input parameters in the simulation software, getting Gaussian, uniform, and Lambertian beams. Each ray will have an associated power, which will depend on the parameters of the input beam. The sum of all the ray powers at the exit of the device will allow us to determine the output power and, therefore, the index of refraction of a liquid placed on the POF.

The maximum number of rays that can travel along the POF is determined by the waveguide parameter $V = 2\pi a(n_{co}^2 - n_{cl}^2)^{1/2}/\lambda$, where $a$ is the radius of the POF (0.49 mm) and $\lambda$ is the wavelength. From this parameter we can calculate that the number of modes that propagate along a highly multimode waveguide is given by $N = V^2/2$ if $V \gg 1$, as happens in our case. If we take into account the values of the refractive indices and the wavelength range (0.4–0.7 μm), $N = 2 \times 10^6$–$3 \times 10^6$. However, this is too large a number of rays to use in developing efficient simulation software. Determining the minimum number of rays to be used in the simulations requires a study of convergence. Such a study, which has already been published,[16] showed that 10.000 rays are enough to reproduce the results (less than 5% of error), which considerably reduces the computation time (by a factor of 100 with respect to the analysis that employs $10^6$ rays).

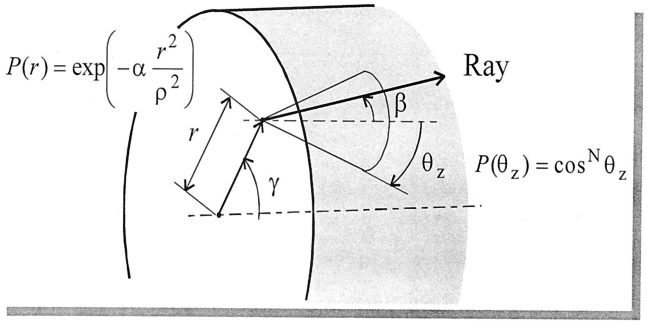


Fig. 2. Transverse view of the POF at the active area, showing the distribution of light foci at the entrance.

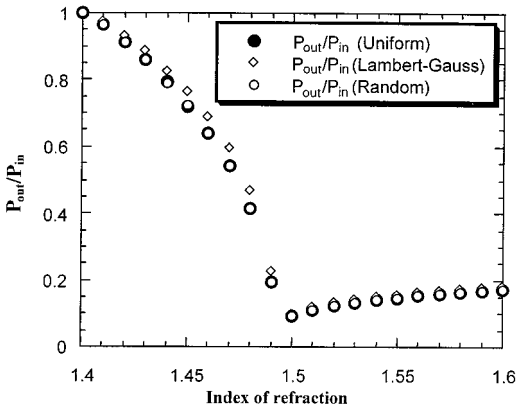


Fig. 3. Relative output power $P_{out}/P_{in}$ of the device for three input power distributions, uniform, Lambertian, and random, for an unbent Eska Extra POF and the following parameters: $L = 3$ cm, $a = 0.49$ mm, $d = 0$, $\rho = \infty$, and $\delta = \infty$.

We also make an analysis of the dependence of the results on the input power distribution. As shown in Fig. 3, the power distribution at the entrance of the device is not critical for good performance. The three different power distributions yield a maximum difference of $5 \times 10^{-3}$ for the values of the index of refraction.

We simulate the effects produced on the polished surface by considering a three-layer system consisting of the POF core, the liquid (whose index of refraction we want to determine), and the surrounding air. Power losses are calculated by means of the reflection and transmission coefficients at the corresponding core–liquid or liquid–air interfaces. The height of the liquid is the most important parameter with which to deduce the amount of lost power. If only a thin layer of liquid is deposited, the rays reflected at the liquid–air interface will go back to the core. A thick liquid layer, however, will cause great power losses, because most of the reflected rays at the interface will no longer enter the core. In this way, one can use the device in one of two ways: by submerging the device in the liquid or by depositing some drops of liquid on the polished section of the fiber.

As the fiber was only slightly curved, we neglect this curvature, which can be justified from our previous results.[16] Parameter $d$ was chosen to be zero (half of the fiber was polished) to maximize the uncovered surface of the core and, therefore, the sensitivity of the device.

In our model we also disregard the influence of the polarization. As was shown previously,[16] the transmission coefficient does not depend significantly on the ray's polarization state. Although the reflection coefficients for two orthogonal polarizations differ by

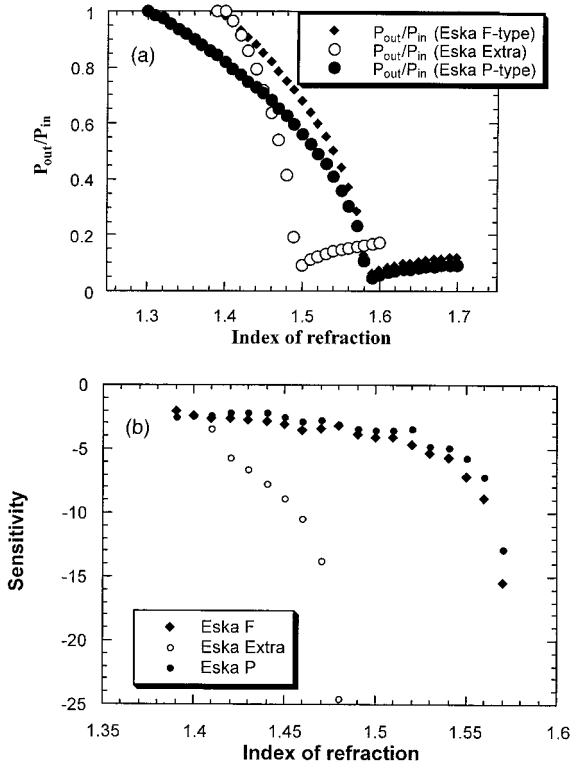


Fig. 4. (a) Relative output power $P_{out}/P_{in}$ as a function of the fiber numerical aperture for $L = 3$ cm, $a = 0.49$ mm, $d = 0$, $\rho = \infty$, and $\delta = \infty$. The results correspond to a Lambertian input power distribution. The numerical apertures of the fibers were Eska F-type, 0.75; Eska Extra, 0.47; and Eska P-type, 0.90. (b) Sensitivity of the device $dP_{rel}/dn$ as a function of the fiber's numerical aperture for the same parameters; $P_{rel} = P_{out}/P_{in}$.

approximately 5% in the worst case (near the critical angle), for a poly(methyl methacrylate) PMMA fiber with $n_{co} = 1.06n_{cl}$ (as in the fibers that we have used), the difference between the results for a device with $L = 3$ cm, $a = 0.49$ mm, $d = 0$, $\rho = 0$, and $\delta = \infty$ is negligible. One of the reasons for this small difference is that the amount of rays at an angle near $\theta_c$ is small, which diminishes the difference to less than 1%. Therefore we use the scalar approximation of the transmission coefficient.[17]

### 3. Results of the Simulation

Intuitively it is possible to infer that, for a liquid whose index of refraction is close to that of the core, the output power will be less than for a liquid with a more distinct refractive index (in the former case, the reflection coefficient at the core–liquid interface is close to zero). Therefore, when the index of the liquid is equal to that of the core, we will have a minimum of output power. It is also possible to deduce that all the liquids whose indices are lower than that of the cladding will yield the same output power, which is maximum, because in such a case all the rays will undergo total internal reflection.

The behavior of the device also depends on the fiber's numerical aperture. Figure 4(a) shows the results for the relative output powers of three POF's of different numerical apertures. In this figure $\delta \sim \infty$; i.e., the device was submerged in the liquid. This means that all the transmitted rays at the core–liquid interface escape from the fiber forever.

As the POF's numerical aperture decreases, the sensitivity $dP_{rel}/dn$ increases, where $P_{rel} = P_{out}/P_{in}$ [see Fig. 4(b)], which makes low-aperture POF's more suitable for use in high-precision devices. If a wide measuring range is necessary, however, high-aperture POF's can be used, although with reduced sensitivity.

Another important feature of the proposed device is the effect of the thickness of the liquid on the output power. In our model we assumed a constant thickness for the covering liquid. If the layer of liquid is thin, the rays reflected at the liquid–air interface will go back to the fiber. On the other hand, we have already mentioned that, for thick liquid layers, rays reflected at the air–liquid interface will no longer enter the fiber. This situation is illustrated in Fig. 5(a). This figure shows that the sensitivity of the device increases strongly with the depth of the liquid because, for shallow liquids and for a fixed length $L$, rays reflected at the air–liquid interface reenter the fiber. As the depth of the liquid increases, there are more rays that cannot enter the fiber, so the difference between input and output powers increases. The minimum for the output power becomes sharper when the depth of the liquid increases.

In Fig. 5(b) the relative output power is plotted as a function of the length of the polished area of the POF. The figure shows that the relative output power decreases as the length increases; the effect is more important for lengths $L$ less than 1 cm and for high-refractive-index liquids. The last property is important if the device is to be used to measure the index of refraction of a liquid whose index of refraction is near that of the POF core. For longer fibers (>1.5 cm), repeatable results are easily obtained.

### 4. Experimental Results and Discussion

In our measurements we used an unjacketed step-index HP-E89328-A fiber (purchased from Hewlett-Packard) of 1-mm diameter whose core was made from PMMA ($n_{co} = 1.492$) and whose cladding was a fluorinated polymer with $n_{cl} = 1.417$. The measuring setup can be described as follows: The beam emerging from a green He–Ne laser ($\lambda = 543.5$ nm) is split into two equal-powered beams in a POF Y coupler. The light from one of the branches is taken as reference, and it is launched into one of the two optical heads of our HP8153A light-wave multimeter. The other branch of the Y coupler is connected to the input of the device under test. The beam travels along the device whose output is led to the second optical head of the multimeter.

We measured semitransparent viscous liquids (Cargille-certified RF 1/5 refractive-index liquids) whose indices of refraction ranged from 1.42 to 1.52. The parameters of the device were $L = 3$ cm, $d = 0$ cm, and $\delta = 0.35 \pm 0.02$ mm. The curvature was large enough to be ignored. We measured the depth

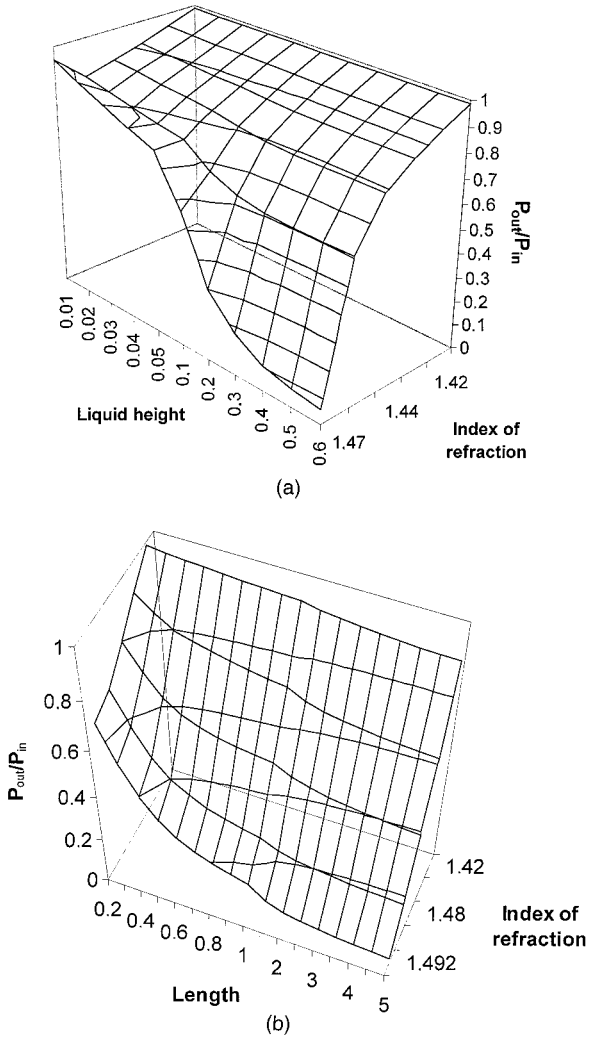


Fig. 5. Results of the simulation. (a) Relative output power as a function of the liquid's refractive index and of the depth of the liquid for $L = 3$ cm, $a = 0.49$ mm, $d = 0$, and $\rho = \infty$. (b) Relative output power as a function of the liquid's refractive index and of the length of the active area for $a = 0.49$ mm, $d = 0$, $\rho = \infty$, and $\delta = \infty$. The results correspond to a Lambertian input power distribution and a PMMA POF with $n_{co} = 1.492$ and $n_{cl} = 1.417$.

of the liquid with a microscope by focusing the light into the upper and lower surfaces of the liquid.

The experimental results are displayed in Fig. 6(a). We can observe that the experimental results corroborate those predicted by our model, with a slight difference for high refractive indices and also in the vicinity of the minimum, which corresponds, as we previously noted, to the refractive index of the core. A glance at Fig. 6(b) shows that a device with a smaller active area ($L = 0.7$ cm, $d = 0$ cm, and $\delta = 0.35$ mm) results in a more pronounced disagreement between simulated and experimental results. This failure is more important at the minimum, where the experimental results yield more output power than expected. It can also be observed that the slope of the experimental results above the minimum is less than was simulated. These two striking differences

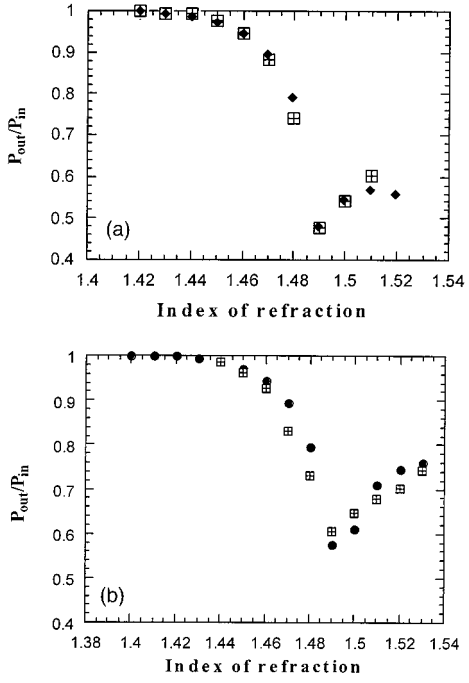


Fig. 6. Comparison of experimental (squares) and simulated (circles) results for a Lambertian input power distribution and for a PMMA POF with $n_{co} = 1.492$ and $n_{cl} = 1.417$: (a) for $L = 3$ cm, $a = 0.49$ mm, $d = 0$, $\delta = 0.35$, and $\rho = \infty$; (b) for $L = 0.7$ cm, $a = 0.49$ mm, $d = 0$, $\delta = 0.35$, and $\rho = \infty$. The size of a square represents the error in the measurement.

for small values of parameter $L$ could be related to our neglect of the curvature of the fiber.

The absolute value of the experimental minimum is larger, however, for the device with $L = 0.7$ cm than for the device with $L = 3$ cm, as was depicted in the simulation results of Fig. 5(b). Then, and as a partial conclusion, we can state that the observed behavior corresponds to that predicted by our model; it is more precise for large values of parameter $L$.

So far we have considered the influence of parameter $L$. Let us consider more carefully the results for different liquid depths. Further insight into the form of Fig. 5(a) for small depths (less than 50 $\mu$m) shows unexpected behavior. This behavior is illustrated in Fig. 7, where the output power is plotted

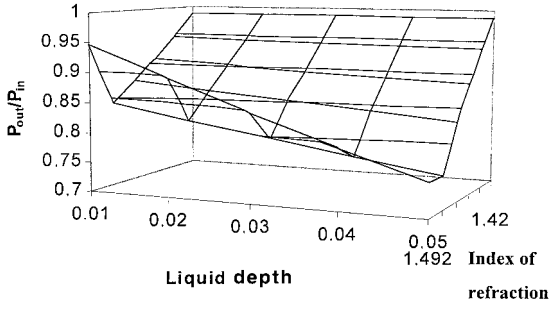


Fig. 7. Relative output power $P_{out}/P_{in}$ as a function of the liquid's refractive index and of the liquid's depth for $L = 3$ cm, $a = 0.49$ mm, $d = 0$, and $\rho = \infty$ and for shallow liquids. The simulation conditions are the same as those for Fig. 5.

against the liquid's depth and refractive index. It can be seen that a relative minimum appears between the values of the cladding and the core refractive indices. Such behavior stems from a trade-off between the transmission coefficient and the number of reflections at the active area. For liquids with refractive indices very close to that of the core (1.492), the number of reflections at the liquid–air interface is small. In such a case the transmission coefficient at the liquid–core interface is the unit, so power losses could be due only either to small changes in the ray paths provoked by discontinuities at the core–liquid and liquid–air boundaries or to the presence of a small number of leaky rays at the input of the device. However, for the moment our model is not able to handle imperfections at both interfaces. However, as the liquid's refractive index diminishes, the liquid retains more and more power, as the power cannot go back to the core because of the discontinuity of the refractive index. Besides, the number of reflections grows, which means that a significant part of the power is lost in faults (small microcracks, voids, etc., . . . ) at the liquid–core interface. The balance of this situation explains the origin of the relative minimum that appears at indices different from that of the core. As the depth of the liquid increases, the number of reflections decreases, and therefore the contribution of the reflections to the power loss is smaller. For a liquid depth of 100 μm, this minimum disappears.

Let us now compare the results of our device with the results that correspond to those for other designs developed for the same purpose. Most of those designs are based on the power lost by an optical fiber when one or several turns are submerged in a liquid of unknown refractive index or when we have a fiber taper.[11–14] Although these designs yield a more nearly linear response over the whole range of refractive indices, obtaining the same sensitivity requires several turns of fiber. The refractometer that we have developed has several advantages. It has a better sensibility for high values of the refractive index (but always under $n_{co}$) as well as better mechanical behavior, because we do not need to bend the fiber, which eliminates variations in the radius of curvature with time that would change the response of the device. Besides, one can use our device in either of two ways: by submerging it into a liquid or by pouring some drops of the liquid on it (an amount necessary to cover the whole sensing area). Previously proposed refractometers require submerging the active part of the fiber in the liquid, so they are not suitable for measurements when the quantity of liquid is small.

For the above reasons we believe that our device is more suitable for mass production than devices proposed previously. We are currently engaged in optimizing the refractometer by modifying the curvature of the fiber at the active area. We are aiming at linearizing the response of the device over the whole measuring range. These results will be reported in a separate paper.

## 5. Conclusions

We have presented a new economical and practical device with which to determine the index of refraction of a liquid. The method combines simplicity of design of the prototypes, ease of connection, and modest price. One can use the device in different configurations either by pouring some drops of liquid onto the polished surface or by immersing the device in the liquid. The resultant accuracy for these two modes of operation is $2 \times 10^{-3}$ and $5 \times 10^{-3}$, respectively, for indices of refraction of 1.30–1.59 (with Eska P-type fiber). This degree of precision is good enough for some of the most popular industrial applications, such as those that produce such liquids as oils, detergents, and juices.

This research is supported by the Departamento de Educación, Universidades e Investigación del Gobierno Vasco of Spain under project UE-1998-4 and also by the Universidad del País Vasco under project UPV 147.345-EA 152/98 ZUBIA. The authors thank López Amo for fruitful discussions.

## References

1. T. Kaino, "Polymer optical fibers," in *Polymers for Lightwave and Integrated Optics: Technology and Applications*, L. A. Hornak, ed. (Marcel Dekker, New York, 1992), pp. 1–38.
2. Y. Koike, T. Ishigure, and E. Nihei, "High-bandwidth graded index polymer optical fiber," J. Lightwave Technol. **13,** 1475–1489 (1995); T. Ishigure, E. Nihei, Y. Koike, C. E. Forbes, L. LaNieve, R. Straff, and H. A. Deckers, "Large core, high-bandwidth polymer optical fiber for near infrared use," IEEE Photon. Technol. Lett. **7,** 403–405, (1995); E. Nihei, T. Ishigure, N. Tanio, and Y. Koike, "Present prospect of graded index plastic optical fiber in telecommunication," IEICE Trans. Electron. **E-80-c,** 117–122 (1997).
3. C. Koeppen, R. F. Shi, W. D. Chen, and A. F. Garito, "Properties of plastic optical fibers," J. Opt. Soc. Am. B **15,** 727–739 (1998).
4. T. F. Stehlin and Y. Liu, "Polymer optical fiber sensors," in *Proceedings of the First International Conference on Plastic Optical Fibers and Applications—POF'92* (Information Gatekeepers, Inc., Boston, Mass., 1992), pp. 124–127.
5. N. Ioannides, D. Kalymnios, and I. W. Rogers, "Experimental and theoretical investigations of a POF based displacement sensor," in *Proceedings of the Second International Conference on Plastic Optical Fibers and Applications—POF'93* (European Institute for Communications and Networks, Geneva, 1993), pp. 162–165.
6. K. Asada and H. Yuuki, "Fiber optic temperature sensor," in *Proceedings of the Third International Conference on Plastic Optical Fibers and Applications—POF'94* (European Institute for Communications and Networks, Geneva, 1994), pp. 49–51.
7. J. D. Weiss, "The pressure approach to fiber liquid-level sensors," in *Proceedings of the Fourth International Conference on Plastic Optical Fibers and Applications—POF'95* (European Institute for Communications and Networks, Geneva, 1995), pp. 167–170.
8. S. Hadjiloucas, D. A. Keating, and M. J. Usher, "Plastic optical fiber sensor for plant water relations," in *Proceedings of the Fifth International Conference on Plastic Optical Fibers and Applications—POF'96* (French Club Fibres Optiques Plastiques, Paris, 1996), pp. 228–237.
9. S. Yamakawa, "Plastic optical fiber chemical sensor with pencil-shaped distal tip fluorescence probe," in *Proceedings of the Sixth International Conference on Plastic Optical Fibers*

*and Applications—POF'97* (Office of Naval Research, Asian Office and POF Consortium, Tokyo, Japan, 1997), pp. 109–110.
10. M. Morisawa, S. Muto, and G. Vishno, "POF sensor for detecting oxygen in air and in water," in *Proceedings of the Seventh International Conference on Plastic Optical Fibers and Applications—POF'98* (International Committee of POF-ICPOF, Germany, 1998), pp. 243–244.
11. B. D. Gupta, and C. D. Singh, "Fiber-optic evanescent field absorption sensor: a theoretical evaluation," Fiber Integr. Opt. **13,** 433–443 (1994).
12. A. L. Harmer, "Optical fiber refractometer using attenuation of cladding modes," in *Proceedings of Optical Fiber Sensors 1* (Institution of Electronics Engineers, London, 1983), pp. 104–108.
13. J. J. Bayle and J. Mateo, "Plastic optical fiber sensor of refractive index, based on evanescent field," in *Proceedings of the Fifth International Conference on Plastic Optical Fibers and Applications—POF'96* (French Club Fibres Optiques Plastiques, Paris, 1996), pp. 220–227.
14. J. Arrue, J. Zubia, G. Fuster, and D. Kalymnios, "Light power behavior when bending POFs," IEE Proc. Optoelectron. **145,** 1–6, (1998); G. Garitaonaindía, J. Zubia, U. Irusta, and J. Arrue, "Passive device based on POF to determine the index of refraction in liquids," in *Proceedings of the Seventh International Conference on Plastic Optical Fibers and Applications—POF'98* (International Committee of POF-ICPOF, Germany, 1998), pp. 178–184.
15. A. Aguirre, U. Irusta, J. Zubia, and J. Arrue, "Fabrication of low loss POF contact couplers," in *Proceedings of the Sixth International Conference on Plastic Optical Fibers and Applications—POF'97* (Office of Naval Research, Asian Office and POF Consortium, Tokyo, Japan, 1997), pp. 132–133; J. Zubia, U. Irusta, J. Arrue, and A. Aguirre, "Design and characterization of a POF active coupler," IEEE Photon. Technol. Lett. **10,** 1578–1580 (1998).
16. A. Ghatak, E. Sharma, and J. Kompella, "Exact paths in bent waveguides," Appl. Opt. **27,** 3180–3184 (1988); J. Arrúe and J. Zubia, "Analysis of the decrease in attenuation achieved by properly bending plastic optical fibers," IEE Proc. Optoelectron. **143,** 135–138 (1996).
17. A. W. Snyder and J. Love, *Optical Waveguide Theory* (Chapman & Hall, London, 1996).